Contribution from the Central Research and Development Department,
E. I. du Pont de Nemours and Company, Experimental Station, Wilmington, Delaware 19898

Synthesis and Properties of Platinum Metal Oxides of the Type $M_xPt_3O_4$

R. D. SHANNON,* T. E. GIER, P. F. CARCIA, P. E. BIERSTEDT, R. B. FLIPPEN, and A. J. VEGA

Received January 12, 1982

Methods were developed for high-yield syntheses of $M_xPt_3O_4$ where M = Li, Na, Mg, Ca, Zn, Cd, Co, and Ni. A new technique involving reaction of a mixture of nitrates and fluorides with PtO_2 gives 60–95% yields based on PtO_2. Another efficient and novel technique is vapor-phase hydrolysis of chloride mixtures. This method produces samples with surface areas of 10–40 m^2/g and has yielded the compositions $H_xPt_3O_{4-y}Cl_y$ and $Ni_xPt_3O_{4-y}Cl_y$, probably the first example of the introduction of H and Cl into the $M_xPt_3O_4$ lattice. Plots of a vs. x are linear for $Na_xPt_3O_4$ and parabolic for $Cd_xPt_3O_4$ while plots of a vs. percent Co, Ni, or Mg are linear for $Co_xNa_yPt_3O_4$, $Ni_xNa_yPt_3O_4$, and $Mg_xNa_yPt_3O_4$, respectively. Magnetic susceptibility and XPS data on $Co_xPt_3O_4$ and $Ni_xPt_3O_4$ suggest the presence of Co^{2+} and Ni^{2+}. Metallic conductivity in $NaPt_3O_4$, $Ni_{0.25}Pt_3O_4$, and $Li_{0.8}Pt_3O_4$ is consistent with short Pt–Pt bonds in the $M_xPt_3O_4$ structure and conflicts with recent claims of semiconducting behavior. $Li_xPt_3O_4$, $Co_xPt_3O_4$, and $Ni_xPt_3O_4$ have high O_2 reduction activity and voltammetric properties similar to those of Pt_3O_4 electrodes.

Introduction

Compounds of the type $M_xPt_3O_4$ are of technological interest because of their use as chlor-alkali anodes[1-7] and H_2–O_2 fuel-cell electrocatalysts. They are also of interest as one of the few examples of oxide families containing Pt^{2+}. Other compounds containing Pt^{2+} are PtO,[8] Na_2PtO_2,[9] $Bi_{1.6}Pb_{0.4}PtO_4$,[10] $K_3Pt_2O_4$,[11] and the family MPt_3O_6, of which $CdPt_3O_6$ is the best characterized.[12,13]

The best characterized member of the $M_xPt_3O_4$ family is $Na_xPt_3O_4$. Its structure was first determined from powder data by Waser and McClanahan[14,15] in 1951 and has recently been confirmed with use of neutron diffraction data.[16] $Na_xPt_3O_4$ shows the unusual feature of Pt–Pt chains running parallel to each of the three cubic axes. The short Pt–Pt distances led Waser and McClanahan to anticipate metallic conductivity. However, lacking sintered samples, they observed semiconducting behavior. They furthermore discovered an electrical polarization effect which they attributed to ionic conductivity caused by sodium ion mobility. They confirmed the presence of Na but did not determine the value of x and on the basis of the work of Galloni and Busch[17] assumed that x is variable from 0 to 1.

In 1972 Cahen et al.[18-21] made an extensive study of the structure, stoichiometry, and physical properties of $M_xPt_3O_4$ compounds (sometimes called platinum bronzes) with M = Na, Cd, and Ni. An excellent summary of the literature on the preparation and characterization of $M_xPt_3O_4$ phases can be found in Cahen's study. In the only single-crystal X-ray study of the "platinum bronze" $Ni_{0.25}Pt_3O_4$, Cahen et al.[18] confirmed the structure described by Waser and McClanahan and with four-probe conductivity measurements confirmed the anticipated metallic conductivity. Cahen et al.[18-21] using the reagents Pt, H_2PtCl_6, and $(NH_4)_2PtCl_6$ also confirmed the existence of $CaPt_2O_4$, $Cd_{0.3}Pt_3O_4$, $Cd_{1.0}Pt_3O_4$, $Na_{0.1}Pt_3O_4$, and $Na_{1.0}Pt_3O_4$ by chemical analysis and neutron diffraction, thereby proving that x could indeed be variable.

Recently Bergner and Kohlhaas[22] and Lazarev and Shaplygin[23,24] have reported the preparation of platinum bronzes with M = Li, Na, K, Mg, Ca, Ba, Zn, Cd, Co, Ni, and Cu using PtO_2 as a reagent. However, the cell dimensions of some of these compounds were not consistent with ionic radii considerations and the phases with M = Mg, Ca, Ba, Zn, Cd, Ni, Co, and Cu were reported by Lazarev and Shaplygin to be semiconductors.[23,24]

Because of the recent discovery that $M_xPt_3O_4$ compositions show activity as H_2–O_2 fuel-cell cathode materials, the need arose for good methods of preparing these materials. The methods used above include reaction of platinum black with metal carbonates,[25] sodium or ammonium chloroplatinates with metal carbonates or nitrates,[14,21,26] and PtO_2 with metal nitrates or carbonates.[22,23] These generally resulted in the desired $M_xPt_3O_4$ product and Pt impurity. Products were purified by heating in aqua regia to dissolve the undesired Pt. Yields are not usually mentioned in most of the above literature, but our experience has been that they are low. One exception was reported by Cahen et al.[21] (hereafter referred to as CIW) who prepared $CaPt_2O_4$ in 100% yield.

The syntheses are specific for each compound. A technique useful for $Li_xPt_3O_4$ does not work for $Na_xPt_3O_4$. The narrow temperature region over which these compounds can be prepared was emphasized by CIW. Another problem probably encountered in most investigations is that PtO_2 frequently contains Na, probably in the form of $Na_xPt_3O_4$. This suggests that most reactions using PtO_2 and metal nitrates or carbonates result in $M_xNa_yPt_3O_4$ rather than $M_xPt_3O_4$ as claimed.

In light of the difficulties described above, we have developed high-yield preparations and report here accurate cell dimensions and electrical conductivities of many $M_xPt_3O_4$ compo-

(1) Thiele, G.; Zöllner, G.; Koziol, K. British Patent 1 328 270, 1973.
(2) Thiele, G.; Zöllner, D.; Koziol, K. U.S. Patent 4 042 484, 1977.
(3) Koziol, K.; Sieberer, H.-H.; Rathjen, H. C. U.S. Patent 3 948 752, 1976.
(4) Zöllner, D.; Zöllner, C.; Koziol, K. U.S. Patent 3 962 068, 1976.
(5) Zöllner, C.; Zöllner, D.; Koziol, K. U.S. Patent 3 992 280, 1976.
(6) Fukuda, M.; Asai, K. German Patent 1 671 455, 1975.
(7) Thiele, G.; Zöllner, D.; Koziol, K. German Patent 1 813 944, 1975.
(8) Westwood, W. D.; Bennewitz, C. D. *J. Appl. Phys.* **1974**, *45*, 2313.
(9) Urland, W.; Hoppe, R. *Z. Anorg. Allg. Chem.* **1972**, *392*, 23.
(10) Boivin, J. C.; Conflant, P.; Thomas, D. *Mater. Res. Bull.* **1976**, *11*, 1503.
(11) Zentgraf, H.; Claes, K.; Hoppe, R. *Z. Anorg. Allg. Chem.* **1980**, *462*, 92.
(12) Shannon, R. D. U.S. Patent 3 663 181, 1972.
(13) Prewitt, C. T.; Schwartz, K. B.; Shannon, R. D., to be submitted for publication in *Acta Crystallogr., Sect. B.*
(14) Waser, J.; McClanahan, E. D. *J. Chem. Phys.* **1951**, *19*, 413.
(15) Waser, J.; McClanahan, E. D. *J. Chem. Phys.* **1952**, *20*, 199.
(16) Schwartz, K. B.; Prewitt, C. T.; Shannon, R. D.; Corliss, L. M.; Chamberland, B. *Acta Crystallogr., Sect. B* **1982**, *B38*, 363.
(17) Galloni, R. E.; Busch, R. H. *J. Chem. Phys.* **1952**, *20*, 198.
(18) Cahen, D.; Ibers, J. A.; Shannon, R. D. *Inorg. Chem.* **1972**, *11*, 2311.
(19) Cahen, D.; Ibers, J. A.; Mueller, M. *Inorg. Chem.* **1974**, *13*, 110.
(20) Cahen, D.; Ibers, J. A. *J. Catal.* **1973**, *31*, 369.
(21) Cahen, D.; Ibers, J. A.; Wagner, J. B. *Inorg. Chem.* **1974**, *13*, 1377.
(22) Bergner, D.; Kohlhaas, R. *Z. Anorg. Allg. Chem.* **1973**, *401*, 15.
(23) Lazarev. V. B.; Shaplygin, I. S. *Russ. J. Inorg. Chem.* (*Engl. Transl.*) **1978**, *23*, 1610.
(24) Lazarev, V. B.; Shaplygin, I. S. *Russ. J. Inorg. Chem.* (*Engl. Transl.*) **1978**, *23*, 291.
(25) Scheer, J. J.; Van Arkel, A. E.; Heyding. R. D. *Can. J. Chem.* **1975**, *33*, 683.
(26) Jorgensen, S. M. *J. Prakt. Chem.* **1877**, *16*, 344.

0020-1669/82/1321-3372$01.25/0

sitions. We also report a preparation of high-surface-area $Li_xPt_3O_4$ and $Ni_xPt_3O_4$ and the results of physical characterization such as magnetic susceptibilities, X-ray photoelectron spectroscopy (XPS), and H NMR measurements.

Experimental Section

Materials. Reagent-grade fluorides, chlorides, carbonates, nitrates, and hydroxides were used. PtO_2 was obtained from Englehard Industries and Comptoir Lyon-Alemand Louyot (CLAL). X-ray analysis of the Engelhard samples generally showed α-PtO_2 and $Na_xPt_3O_4$. The CLAL sample showed only broad lines of α-PtO_2. Analysis of an Engelhard sample showing only a trace of $Na_xPt_3O_4$ indicated 0.66% Na, which was reduced to 0.56% by heating 24 h in aqua regia. Emission spectrographic analysis showed the additional presence of Ni, Fe, Mg, Ca, and Si at the 500–2500-ppm level, B, Cr, and Cu at the 200–1000-ppm level, Al and Mn at the 100–500-ppm level, and Pb at the 50-250-ppm level. Thermogravimetric analyses (TGA) in air showed weight loss beginning at ~580 °C and ending at 650 °C.

Analysis of the CLAL sample at first gave 0.99% Na, after 18 h in hot aqua regia, 0.36%, and after a second 18-h treatment, 0.13%. Emission spectrographic analysis of this PtO_2 gave the following: Ca, 200–1000 ppm; B, Cr, Fe, Ni, Mg, Si, and Pb, 50–250 ppm, and Rh, 20–100 ppm.

Analytical Techniques. $M_xPt_3O_4$ samples were analyzed for Li, Na, Mg, Ca, Zn, Cd, Ni, or Co by atomic absorption after first being dissolved in hot 48% HBr. Oxygen analyses were obtained by a catalytic fusion method using a LECO Nitrox 2400c unit. X-ray diffraction patterns were obtained with a Guinier-Hägg focusing camera (r = 40 mm). The radiation was monochromatic Cu $K\alpha_1$ (λ = 1.54051 Å). KCl (a = 6.2931 Å) was used as an internal standard. Line positions on the film were determined to ±5 μm with a David Mann film reader; intensities were estimated by oscilloscopic comparison of film density with the strongest line of the pattern. Cell dimensions were obtained by least-squares refinement of "d" values. High-temperature X-ray patterns (HTG) were obtained with a Nonius Guinier camera. Differential thermal analyses (DTA) and TGA scans were made with a Du Pont thermal analyzer. Four-probe resistivity measurements were made according to a technique described earlier.[27] The photoelectron spectra were obtained on a Du Pont 650B spectrometer, equipped with a nondispersive filter analyzer, a magnesium anode, and a Nicolet Model 1072 multichannel analyzer for data acquisition. The powdered samples were mounted on a sample probe with double-sided adhesive tape. The spectra were smoothed via a nine-point Savitsky–Golay smoothing routine and background corrected, and the binding energies and peak areas were obtained. These peak areas were normalized with use of the photoelectric cross sections of Scofield,[28] and atomic ratios were calculated from these normalized values. The values of binding energies (E_B) of the photoelectrons were charge corrected to oxygen by assigning 530.6 eV to the dominant O 1s peak. Magnetic measurements were made on 5–80-mg powder samples with a Faraday balance in fields of 500–7000 Oe between 128 and 475 K.

Proton NMR experiments were carried out at 90 MHz with a Bruker SXP100 spectrometer. Proton concentrations were determined from the intensity of the free induction decay following a 90° pulse on resonance. The signal intensity was calibrated with a weighed sample of H_2O diluted in D_2O, with care taken to correct the spurious background signals. Line widths were measured as the full width at half-maximum of the Fourier-transformed spectra taken off resonance. In addition, Carr–Purcell–Meiboom–Gill[29] and REV-8 multiple-pulse[30] experiments were performed to determine the contributions of various broadening mechanisms to the line width: the Carr–Purcell spin echo decay rate has no contributions from chemical shift, paramagnetic susceptibility, and heteronuclear dipolar interactions. On the other hand, multiple-pulse line-shape measurements suppress homonuclear dipolar interactions, while the multiple-pulse relaxation rates, T_{1xz},[31] contain no contributions from any of these static interactions but rather reflect homogeneous broadening due to molecular motions. Experimental details of the multiple-pulse experiment have been described elsewhere.[32]

Paramagnetic susceptibilities were measured with use of a coaxial arrangement of NMR tubes with the platinum compound in the inner tube (5 mm o.d.) surrounded by acetone in the outer tube (7.5 mm o.d.). In this method,[33] the splitting of the acetone signal is a direct measure of the volume susceptibility.

Electrodes of $Li_xPt_3O_4$, $Ni_xPt_3O_4$, and $Co_xPt_3O_4$ were prepared as thin $^1/_2$ in. diameter disks of platinum oxide powder mixed with 2 wt % of a binder of Teflon 6 fluorocarbon resin and pressed at 40000 psi at room temperature. Electrical contact was made by a Au wire attached with conductive Ag epoxy to one side of the disk sputter coated with Au. This side was later sealed with epoxy to a glass tube threaded with the Au wire. Thus, only one face of the disk (~1 cm^2) was exposed to the electrolyte. Typical electrical resistance between electrode faces was ~1 Ω.

Electrochemical measurements were made with a Princeton Applied Research Model 173 potentiostat/galvanostat. It was driven by waveforms from its companion PAR Model 175 universal programmer. The reference was a dynamic hydrogen electrode.[34] It was compared to a saturated calomel (SCE) electrode and found to agree within a maximum of 50 mV. All measured potentials are given vs. the dynamic hydrogen electrode (DHE); all other potentials are expressed vs. the normal hydrogen electrode (NHE).

Synthesis. The flux method using a LiCl–KCl eutectic is successful for preparation of $Li_xPt_3O_4$ but not for other members of the series. Reaction of Pt with a carbonate works only for Na. The reaction of PtO_2 with nitrates is successful for many compositions but is a low-yield reaction. An efficient preparation for some bronzes is vapor-phase hydrolysis of chloride mixtures. Another process suggested by the preparation of $Pt_{0.4}Pt_3O_4$[35] using KF, CuO, and CaO in a Pt crucible is the reaction of PtO_2 with fluoride–nitrate mixtures. Although the reactions involving PtO_2 are most efficient, they generally do not yield compositions free of Na because of Na impurity in PtO_2. Thus, most of the compositions with PtO_2 as a reagent are $M_xNa_yPt_3O_4$.

Vapor-phase hydrolyses of chloride mixtures are particularly useful in preparing high-surface-area materials. This approach to preparing high-surface-area platinum bronzes involves exposing a powdered metal hexachloroplatinate(IV) in a ceramic boat to flowing vapors of either HNO_3 or H_2O at 300–500 °C at ambient pressure. The boat is placed in a horizontal quartz tube in a suitably controlled electric tube furnace. The HNO_3–H_2O atmosphere is established by introducing the liquid dropwise into the tube, with subsequent exhaustion to the atmosphere after vaporizing through the hot zone. Under these conditions HNO_3 is essentially completely decomposed to NO_2, O_2, and H_2O.

The powdered starting material is prepared by dissolving a weighed quantity of platinum metal in aqua regia and adding the amount of metal chloride or carbonate necessary to give the required metal/platinum molar ratio in solution. The clear solution is evaporated to dryness and ground up under nitrogen. Under these conditions, the stoichiometry of the starting material is $M^n_{(2-x)/n}H_xPtCl_6 \cdot yH_2O$. Retention of nitrate and/or chloride ion is possible in synthesis. Repeated solution and reevaporation of starting material from concentrated HCl effectively removes the nitrate ion, but the product of the final low-temperature hydrolysis does not change. This process is superior to heating the hexachloroplatinates in air or oxygen since the presence of H_2O or HNO_3 vapors permits a reaction temperature about 100 °C lower, and the product bronzes are more uniform, with higher surface area. However, difficulties with polyphase products are encountered in some systems, notably the Li–Pt–O system, and high yields of the desired bronzes may require more adequate control of the redox conditions. Furthermore, because of the broad X-ray lines, it is not possible to obtain accurate cell dimensions.

$Li_xPt_3O_4$. A particularly effective way of preparing $Li_xPt_3O_4$ involves the use of PtO_2 in a LiCl–KCl flux according to a process described by Thiele et al.[2] and modified to improve the yield. The literature procedure called for the slow addition of PtO_2 powder to the molten flux at 400 °C; however, our X-ray and scanning electron microscope (SEM) analyses of the product indicate that this process

(27) Bither, T. A.; Gillson, J. L.; Young, H. S. *Inorg. Chem.* **1966**, *5*, 1559.
(28) Scofield, J. H. *J. Electron Spectrosc.* **1976**, *8*, 129.
(29) Mehring, M. *NMR: Basic Princ. Prog.* **1976**, *11*.
(30) Rhim, W.-K.; Elleman, D. D.; Vaughan, R. W. *J. Chem. Phys.* **1973**, *59*, 3740.
(31) Vega, A. J.; Vaughan, R. W. *J. Chem. Phys.* **1978**, *68*, 1958.
(32) Vega, A. J.; English, A. D. *Macromolecules* **1980**, *13*, 1635.
(33) Orrell, K. G.; Sik, V. *Anal. Chem.* **1980**, *52*, 567.
(34) Giner, J. *J. Electrochem. Soc.* **1964**, *111*, 376.
(35) Grande, B.; Muller-Buschbaum, H. *J. Inorg. Nucl. Chem.* **1977**, *39*, 1084.

resulted in rapid surface reaction of PtO_2 and a subsequent agglomeration of the PtO_2–$Li_xPt_3O_4$ mixture. This was eliminated by thoroughly mixing the components before heating the mixture to 400 °C in air. Typically, 19 g of PtO_2, 46.0 g of LiCl, and 53.9 g of KCl were placed in an Al_2O_3 crucible, heated at 480 °C for 6 h and 600 °C for 12 h, and cooled slowly to room temperature. The chlorides were dissolved with H_2O and then HCl. The product, a black powder mixed with metallic Pt crystals, was then ground and boiled in aqua regia for 48 h to remove the Pt. X-ray diffraction revealed single-phase cubic $Li_xPt_3O_4$ with $a = 5.620$ Å. SEM showed the product to consist of cubic crystals approximately 1 μm on an edge. Quantitative analysis indicated 0.847% Li, 500 ppm Na, 89.35% Pt, and 9.77% O corresponding to the composition $Li_{0.8}Pt_3O_4$.

Analysis of another sample of $Li_xPt_3O_4$ prepared from LiCl–KCl flux showed 0.78% Li, 200–1000 ppm Na, and 9.46% O, compared to the calculated values for $Li_{0.8}Pt_3O_4$ of 0.85% Li and 9.77% O. The stability in H_3PO_4 was evaluated. After 314 h in 96% H_3PO_4 at 180 °C there was no significant change in the composition, 0.8% Li and 9.34% O. Because several investigators have hypothesized the existence of $H_xPt_3O_4$, H analysis was also carried out. No H was found within a detection limit of 0.04%. The hydrogen content of an untreated sample of $Li_{0.8}Pt_3O_4$ was determined by NMR to be 0.06% H. After the sample was heated for 16 h at 200 °C under high vacuum, no proton signal was observed. There was thus less than 5 ppm H, which corresponds to $H_{<0.003}Li_{0.8}Pt_3O_4$.

When the LiCl–KCl–PtO_2 flux procedure is used, low reaction temperatures (400–500 °C) generally yielded a product containing PtO_2 as an impurity. With higher temperatures, 550–625 °C, there was the tendency to produce some Pt impurity. PtO_2 was removed by treatment with oxalic acid. This treatment converted the PtO_2 to Pt, which was removed with boiling aqua regia (4–16 h). While it was possible to remove Pt and/or PtO_2 by posttreatment of the preparation, it is not desirable to do so because of the possible effect of these reagents on the $Li_{0.8}Pt_3O_4$ surface area. Typically samples having surface areas of 2–4 m^2/g are produced by the flux method.

DTA of the flux-prepared $Li_{0.8}Pt_3O_4$ showed decomposition beginning at ~750 °C and peaking at 840 °C. TGA in vacuum indicated weight loss beginning at 500 °C and ending at 850 °C (~9.0% weight loss). As a test of the stability of $Li_xPt_3O_4$, a sample produced in the LiCl–KCl reation was held at 500 °C for 7 days. Li analysis showed a loss of Li to give the composition $Li_{0.63}Pt_3O_4$.

Preparations involving mixtures of 0.5 LiF, 0.5 $LiNO_3$, and 3 PtO_2 (numbers refer to mole ratios throughout) were made by thoroughly grinding and pelletizing the reagents, slowly heating in an Al_2O_3 crucible to 700 °C, holding for 4 h, regrinding, repelletizing, and reheating at 700 °C for 16 h. The samples were heated for 24 h in aqua regia to remove unreacted Pt and other possible impurities. This technique produces a pure $Li_xPt_3O_4$ phase with a yield of ~80% based on PtO_2. Anal. Calcd for $Li_{0.63}Pt_3O_4$: Li, 0.67; O, 9.79. Found: Li, 0.67; O, 9.48. Fluorine analysis showed <0.2%.

Ceramic pellets $^1/_4$ in. diameter by $^1/_4$ in. thick were prepared from this material after sealing in a Pt capsule and heating at a pressure of 10 kbar and temperature of 725 °C for 1 h followed by cooling 100 °C/h to room temperature. This pellet was dense, well sintered, and suitable for resistivity measurements (see below).

Hydrothermal preparations in sealed Au or Pt tubes with PtO_2, $LiOH·H_2O$, and $KClO_3$ generally resulted in yellow Li_2PtO_3. Omission of $KClO_3$ yields $Li_xPt_3O_4$ and weak to moderate spinel and PtO_2 impurities. Introduction of small amounts of NH_4OH gave a similar result.

The vapor-phase hydrolysis method is particularly suited to the preparation of high-surface-area $Li_xPt_3O_4$. Mixtures of lithium and platinum chlorides were prepared in the usual way (Li/Pt = 4/1 to 1/3) and exposed to different oxidation–hydrolysis conditions at 350–500 °C. The products were quite sensitive to not only the Li/Pt ratio in the starting chlorides but also the p_{O_2} existing in the furnace. For example, heating Li_2PtCl_6 under steam for 5 days at 450 °C yielded a mixture of 2 cubic bronzes, Pt_xO (vide infra), LiCl, and probably Li_2PtO_3. Heating this crude product to 650 °C for 1 h followed by an aqua regia treatment gave a product with two bronze patterns ($a = 5.62$ Å major, 5.65 Å minor) in nearly 90% yield with a surface area of 1 m^2/g. Under HNO_3 vapor at 450–500 °C, Li_2PtCl_6 tends to form more of the Li_2PtO_3 phase and less of the bronze.

Reducing the ratio Li/Pt to 1/3 and/or using $HgCl_2$ as a fugitive mineralizer minimized the production of a second cubic form of bronze but did not eliminate the concurrent production of Pt_xO, which could only be removed by a heat treatment at 650 °C and a subsequent aqua regia wash. A preferred synthesis of $Li_xPt_3O_4$ consists of heating a mixture of LiCl–$HgCl_2$–$PtCl_4$ in 1/2/3 molar ratio under steam at 425 °C overnight. The product (77% yield) after treatment with warm aqua regia to remove Pt metal consisted of a single cubic phase ($a = 5.65$ Å) with a surface area of 7–10 m^2/g and a Li content of 0.65–0.70%.

$NaPt_3O_4$. A hydrothermal technique proved most successful in the preparation of $NaPt_3O_4$. A mixture of 0.5 g of PtO_2, 0.2 g of NaOH, 0.25 g of $KClO_3$, and 2 cm^3 of H_2O was sealed in a Pt tube 5 in. long by $^3/_8$ in. diameter and heated at 700 °C and 3000 atm for 24 h and quenched. The product was found to be single-phase cubic $Na_xPt_3O_4$ ($a = 5.687$ Å). SEM indicated crystallites with cubic morphology approximately 0.8–1.0 μm on an edge. Chemical analysis of the product showing 3.52% Na, 87.54% Pt, and 8.76% O corresponds closely to $NaPt_3O_4$ with 3.42% Na, 87.06% Pt, and 9.52% O. This sample was not attacked by H_3PO_4 at 180 °C; an analysis after 427-h exposure showed 3.53% Na, 87.03% Pt, and 9.2% O.

An attempt to use a NaCl–$NaNO_3$ flux similar to that used for $Li_xPt_3O_4$ produced $Na_xPt_3O_4$ and a large amount of Pt, which could not be removed after three successive treatments in hot aqua regia. Conditions to prepare $Na_xPt_3O_4$ from Na–Pt–Cl precursors by hydrolysis were not found. Heating Na_2PtCl_6 to 435 °C under steam over a 3-day period yielded a platinum oxide approximately Pt_3O_4 in about 40% yield. Anal. Calcd for Pt_3O_4: Pt, 90.14; O, 9.86. Found: Pt, 88.38; O, 9.42; Na, 0.17; Cl, 1.4.

The material is a semiconductor, has a surface area of 10–20 m^2/g, and is insoluble in aqua regia. It is attacked slowly by hot H_3PO_4.

$Mg_xNa_yPt_3O_4$. A mixture of 0.5 MgF_2, 0.5 $Mg(NO_3)_2·6H_2O$ and 3.0 α-PtO_2 was thoroughly ground, pelletized, placed in an Al_2O_3 crucible, and heated at 100 °C for $^1/_4$ h, 450 °C for $^1/_2$ h, 500 °C for $^1/_2$ h, 550 °C for $^1/_2$ h, and 600 °C for 4 h. The pellet was then reground, repelletized, and heated at 650 °C for 14 h. The product was treated in hot aqua regia for 24 h to dissolve any unreacted magnesium oxides and Pt. The black product (yield 25%) was single-phase $(Na,Mg)_xPt_3O_4$ with $a = 5.6392$ Å. Analysis for Na and Mg yielded Na = 0.49% and Mg = 1.03% and corresponds to $Mg_{0.28}Na_{0.14}Pt_3O_4$. The electrical resistivity of a compressed disk was 126 Ω cm.

A reaction similar to the above but with only $Mg(NO_3)_2·6H_2O$ yielded the product $Na_{0.77}Mg_{0.13}Pt_3O_4$ with $a = 5.6774$ Å. Cell dimensions for both of these $Mg_xNa_yPt_3O_4$ compositions are in reasonable agreement with an approximate Vegard relationship using 5.687 Å for $NaPt_3O_4$ and 5.621 Å for $Mg_xPt_3O_4$.[36]

$K_xPt_3O_4$. Although $K_xPt_3O_4$ was reported by both Bergner and Kohlhaas[22] (hereafter referred to as BK) and Lazarev and Shaplygin[23] (hereafter referred to as LS), we have been unable to prepare it by the hydrothermal technique or by reaction of PtO_2 with fluoride–nitrate–carbonate mixtures. Small amounts of a $M_xPt_3O_4$ phase with $a = 5.67$ Å were obtained in agreement with the above authors, but this is probably $Na_xPt_3O_4$.

$Ca_xPt_3O_4$. Cahen's preparation[21] for $CaPt_2O_4$ using $CaCO_3$ and $(NH_4)_2PtCl_6$ was repeated with good results. $CaPt_3O_4$ was prepared from a mixture of 1.0 $Ca(NO_3)_2·4H_2O$ and 3.0 PtO_2 at 650 °C and subsequent purification in aqua regia. Analysis of the product (yield 73%) gave Ca = 5.93% and Na = 0.22% and corresponds to $Ca_{1.02}Na_{0.06}Pt_3O_4$. The cell dimension, $a = 5.7413$ Å, agrees well with that of BK ($a = 5.733$ Å) and LS ($a = 5.743$ Å).

A similar reaction with CaF_2, $Ca(NO_3)_2·4H_2O$, and PtO_2 at 600 °C produced $Ca_{0.54}Na_{0.17}Pt_3O_4$ with $a = 5.6991$ Å and a yield of only 15% after 24 h in aqua regia.

$Co_xNa_yPt_3O_4$. The reaction of 1.2 $Co(NO_3)_2·6H_2O$ and 3.0 PtO_2 at 650 °C for 16 h produced a composition which was analyzed to be 2.11% Na and 1.91% Co, corresponding to $Na_{0.61}Co_{0.22}Pt_3O_4$. The cell dimension ($a = 5.6726$ Å) is consistent with this solid solution.

A similar reaction but utilizing 1.0 cobalt nitrate and 3.0 PtO_2 resulted in $PtCoO_2$ (yield 12%). This material had previously been prepared only in sealed tubes by metathesis or at elevated pressures.[37] The use of 0.5 CoF_2, 0.5 $Co(NO_3)_2·6H_2O$, and 3 PtO_2 and a temperature of 700 °C increased the yield of $PtCoO_2$ to 56%.

It was, however, possible to prepare $Co_xNa_yPt_3O_4$ compositions by using mixtures of NaF, CoF_2, $Co(NO_3)_2·6H_2O$ and PtO_2. For

(36) Muller, O.; Roy, R. *Adv. Chem. Ser.* **1971**, *No. 98*, 28.
(37) Shannon, R. D.; Rogers, D. B.; Prewitt, C. T. *Inorg. Chem.* **1971**, *10*, 713.

Table I. Cell Dimensions, Oxygen Analyses, and Resistivities

a. $M_xPt_3O_4$

composition	cell dimens, A	% O found	% O calcd	ρ(298 K), Ω cm	temp dependence	sample form
$Li_{0.80}Pt_3O_4$	5.6200 (2)	9.4, 9.5	9.77	1.0×10^{-4}	+	*a*
$Li_{0.63}Pt_3O_4$	5.6227 (4)	9.5	9.79			
$Li_{0.73}Na_{0.07}Pt_3O_4$	5.6242 (2)					
$NaPt_3O_4$	5.6870 (2)	8.8, 8.9	9.52	9×10^{-5}	+	*b*
$Ca_{0.54}Na_{0.17}Pt_3O_4$	5.6991 (10)					
$Ca_{1.0}Na_{0.05}Pt_3O_4$	5.7413 (7)					
$Mg_{0.13}Na_{0.77}Pt_3O_4$	5.6774 (4)			126		*c*
$Mg_{0.28}Na_{0.14}Pt_3O_4$	5.6392 (4)					
$Zn_{0.63}Na_{0.08}Pt_3O_4$	5.6356 (3)					
$Cd_{0.40}Pt_3O_4$	5.6673 (5)					
$Cd_{0.20}Na_{0.44}Pt_3O_4$	5.6924 (3)			13		*c*
$CaPt_2O_4$ (tetragonal)	5.788 (1), 5.601 (2)					
$Co_{0.21}Na_{0.61}Pt_3O_4$	5.6726 (7)					
$Co_{0.45}Na_{0.28}Pt_3O_4$	5.6377 (4)	8.8	9.38			
$Co_{0.38}Na_{0.30}Pt_3O_4$	5.6411 (7)					
$Co_{0.34}Na_{0.14}Pt_3O_4$	5.6321 (4)	8.8	9.52			
$Co_{0.50}Na_{0.15}Pt_3O_4$	5.6381 (3)					
$Co_{0.50}Na_{0.21}Pt_3O_4$	5.6497 (9)					

b. $Ni_xNa_yPt_3O_4$

composition	cell dimens, A: Ni rich	cell dimens, A: Na rich	% O found	% O calcd	ρ(298 K), Ω cm	temp dependence	sample form
$Ni_{0.08}Na_{0.80}Pt_3O_4$	5.6794 (5)						
$Ni_{0.20}Li_{0.19}Pt_3O_4$	7.945 (4) 9.842 (5)	5.654 (9)					
$Ni_{0.22}Na_{0.30}Pt_3O_4$	7.952 (5) 9.860 (9)	5.659 (7)	9.3	9.56			
$Ni_{0.26}Na_{0.27}Pt_3O_4$	7.943 (7) 9.849 (12)	5.664 (7)	9.4	9.53			
$Ni_{0.28}Na_{0.15}Pt_3O_4$	5.6229 (5)	5.634 (7)					
$Ni_{0.32}Na_{0.23}Pt_3O_4$	7.950 (9) 9.85 (2)	5.661 (9)					
$Ni_{0.37}Na_{0.37}Pt_3O_4$	5.6342 (8)						
$Ni_{0.38}Na_{0.38}Pt_3O_4$	5.6339 (8)	5.647 (6)					
$Ni_{0.38}Na_{0.22}Pt_3O_4$	5.6307 (5)				2×10^{-4}	+	*c*
$Ni_{0.40}Na_{0.26}Pt_3O_4$	5.6290 (5)						
$Ni_{0.47}Na_{0.34}Pt_3O_4$	5.6348 (6)						
$Ni_{0.46}Na_{0.21}Pt_3O_4$	5.6256 (5)		9.0	9.40			
$Ni_{0.52}Na_{0.12}Pt_3O_4$	7.911 (2) 9.826 (3)	5.646 (6)					
$Ni_{0.51}Na_{0.15}Pt_3O_4$	7.927 (3) 9.803 (4)	5.639 (6)					
$Ni_{0.50}Na_{0.06}Pt_3O_4$	7.900 (1) 9.804 (1)						
$Ni_{0.53}Na_{0.08}Pt_3O_4$	7.909 (2) 9.830 (3)	5.641 (8)	9.9	9.38			

[a] Sintered pellet. [b] Single crystal. [c] Compressed powder.

example, a mixture of 0.5 NaF, 0.25 CoF_2, 0.25 $Co(NO_3)_2 \cdot 6H_2O$, and 3 PtO_2 heated at 600 °C for 16 h produced $Co_{0.50}Na_{0.15}Pt_3O_4$ (Co = 4.37%, Na = 0.05%, yield 91%, a = 5.6381 Å). Fluorine analysis gave <0.2%.

Hydrothermal preparation utilizing Co_3O_4, PtO_2, and NH_4OH resulted in $Co_xPt_3O_4$, PtO_2, and Pt. Similarly, vapor-phase hydrolysis was not successful in the preparation of $Co_xPt_3O_4$. Heating Co–Pt–Cl mixtures under steam or HNO_3 gave only the spinel $(Co,Pt)_3O_4$ and platinum metal. Neither the bronze $Co_xPt_3O_4$ nor the delafossite $CoPtO_2$ was detected under these conditions.

$Ni_xNa_yPt_3O_4$. A mixture of 0.25 NaF, 0.50 NiF_2, 0.25 $Ni(NO_3)_2 \cdot 6H_2O$, and 3 PtO_2 heated at 600 °C for 16 h gave a black product (yield 79%) which was analyzed to be 4.47% Ni and 0.40% Na, corresponding to $Ni_{0.52}Na_{0.12}Pt_3O_4$. Other ratios of reactants yielded slightly different compositions listed in Table Ib.

In contrast to other members of the series the presence of nickel nitrate does not appear to be essential to a good yield. A mixture of 1.0 NiF_2 and 3.0 PtO_2 heated at 650 °C under flowing O_2 for 16 h produced a composition that was analyzed to be 4.53% Ni and 0.27% Na, corresponding to $Ni_{0.53}Na_{0.08}Pt_3O_4$. Ratios of NiF_2 and PtO_2 other than 1/3 produced the $Ni_xNa_yPt_3O_4$ phases and an unidentified phase thought to be $PtNiO_2$.

The X-ray diffraction patterns of most of these compositions showed splittings characteristic of distorted-cubic symmetry. In most of the 16 different $Ni_xNa_yPt_3O_4$ samples doublet splitting of all lines except 110, 200, and 222 occurred. This ruled out the presence of two cubic phases and suggested that the Ni compounds could be hexagonal with $a \simeq 7.9$ and $c \simeq 9.8$ Å. However, occasional splitting of the 200 and 400 lines into doublets and the 210, 320, and 321 lines into triplets suggested either a symmetry lower than hexagonal or the presence of two phases.

A high-resolution SEM photograph[38] taken of apparently cubic $Ni_{0.46}Na_{0.21}Pt_3O_4$ crystals that had been etched with aqua regia showed a peculiar "jigsaw puzzle" surface with light-colored islands about 200 Å in diameter in a darker matrix. This feature, suggestive of a two-phase system, was corroborated by analyses of these crystals by X-ray emission spectroscopy with a Vacuum Generator HB-501

(38) McKinnon, I., personal communication.

STEM.[39] Crystal fragments 200–2000 Å in length showed regions having Pt/Ni = 9–11 and other regions having Pt/Ni $\simeq$ 4.

In light of these results, we believe the $Ni_xNa_yPt_3O_4$ compositions consist of two phases: (1) a hexagonal Ni-rich phase and (2) a cubic Na-rich phase. Table Ib summarizes the properties of the $Ni_xNa_yPt_3O_4$ compositions. The X-ray patterns of most of the compositions with $x \lesssim 0.3$ and ~ 0.5 clearly show the hexagonal splitting. The intermediate compositions, in spite of their apparent cubic single-phase X-ray pattern, appear to be two-phase mixtures, as evidenced by the STEM analysis of $Ni_{0.46}Na_{0.21}Pt_3O_4$. Evidently, the compositional domains are too small to observe the splitting.

Hydrothermal treatment using $Ni(OH)_2$, PtO_2, and $KClO_3$ at 600 °C and 2000 atm produced only NiO and PtO_2. Omission of $KClO_3$ resulted in an unidentified, highly resistive phase. Inclusion of NH_4OH resulted in $M_xPt_3O_4$ and PtO_2.

A solid-state reaction of 0.6 NiO and 3.0 PtO_2 in a sealed Pt tube at 850 °C and 3 kbar resulted in a black product containing 2.29% Ni and 0.59% Na, corresponding to $Ni_{0.26}Na_{0.17}Pt_3O_4$. The X-ray diffraction pattern was indexed on a hexagonal cell with a = 7.931 Å and c = 9.779 Å.

A high-surface-area nickel platinum oxide was successfully prepared by vapor-phase hydrolysis. Varying the initial Ni/Pt ratio and the hydrolysis conditions over a wide range resulted in the following optimum procedure for the preparation of this phase. A mix of nickel and platinum chlorides in a 0.4/3 ratio was heated under a stream of water-saturated O_2 at 425 °C for 3–4 days. The black powder (95% yield) had a surface area of 41 m^2/g and a cell edge of 5.68 Å. Similar preparations gave analyses for $Ni_xPt_3O_4$ (x = 0.28 → 0.50), but chloride ion was also always present in small amounts (ca. 1–2%). On the basis of the Cl content and the cell dimension, we believe the composition to be $Ni_xPt_3O_{4-y}Cl_y$. In an NMR measurement of one of these samples with the composition $Ni_{0.5}Pt_3O_{4-y}Cl_y$, the hydrogen content was found to be 0.03% H. After the sample was heated for 16 h at 200 °C under high vacuum, no proton signal was observed. Thus, there was less than 5 ppm H, which corresponds to $H_{<0.003}Ni_{0.5}Pt_3O_{4-y}Cl_y$.

$Zn_xNa_yPt_3O_4$. Reaction of 1.0 $Zn(NO_3)_2 \cdot 6H_2O$ and 3.0 PtO_2 at 650 °C for 16 h resulted in a $Zn_xNa_yPt_3O_4$ phase with a = 5.675 Å. Reaction of 0.5 ZnF_2, 0.5 $Zn(NO_3)_2 \cdot 6H_2O$, and 3.0 PtO_2 at 600 °C for 16 h resulted in a $Na_xZn_yPt_3O_4$ phase (yield 59%) that was analyzed to be 5.92% Zn and 0.26% Na, corresponding to $Zn_{0.63}Na_{0.08}Pt_3O_4$.

Vapor-phase hydrolysis was not successful in preparing $Zn_xPt_3O_4$. Heating $ZnPtCl_6$ to 425 °C under either steam or HNO_3 overnight gave primarily the spinel $(Zn,Pt)_3O_4$ (a = 8.60 Å) with trace quantities of either the zinc or another bronze. Other unidentified phases were also present in small amounts.

Attempts to prepare $Zn_xPt_3O_4$ hydrothermally from ZnO, PtO_2, and $KClO_3$ resulted in PtO_2 and $(Zn,Pt)_3O_4$ spinel. Omission of $KClO_3$ and introduction of NH_4OH resulted in a mixture of PtO_2 and $(Na,Zn)_xPt_3O_4$.

$Sr_xPt_3O_4$ and $Ba_xPt_3O_4$. Reaction of 1 $Sr(NO_3)_2$ with 3 PtO_2 at 650 °C gave an amorphous product. BK and LS were also unable to prepare $Sr_xPt_3O_4$.

Reaction of 1.0 $Ba(NO_3)_2$ with 3.0 PtO_2 resulted in a $Ba_xNa_yPt_3O_4$ phase (yield 10%) with a = 5.692 Å in good agreement with the value of 5.690 Å proposed by BK and somewhat smaller than that of LS of 5.715 Å. However, analysis of this phase resulted in 3.23% Na and 0.14% Ba, corresponding to $Na_{0.67}Ba_{0.01}Pt_3O_4$.

A similar reaction using 0.5 BaF_2, 0.5 $Ba(NO_3)_2$, and 3.0 PtO_2 resulted in a phase with a = 5.676 Å (yield 1%). On the basis of these results and a lack of success in preparing $Sr_xPt_3O_4$ we conclude that $Ba_xPt_3O_4$ cannot be prepared and that previous investigators have prepared $Na_xBa_yPt_3O_4$ where $y << x$.

$Ag_xPt_3O_4$. A reaction of 2.0 $AgNO_3$ and 1.0 PtO_2 produced a phase (yield 18%) that was analyzed to be $Na_{0.73}Ag_{0.02}Pt_3O_4$ with a = 5.689 Å. Another reaction utilizing 0.5 NaF, 0.5 $AgNO_3$, and 3.0 PtO_2 produced a phase (yield 64%) that was analzyed to be $Na_{0.84}Ag_{0.004}Pt_3O_4$ with a = 5.6792 Å. From these results it seems unlikely that much Ag can enter into the $M_xPt_3O_4$ structure in fluoride–nitrate–PtO_2 reactions.

$Cd_xPt_3O_4$. $Cd_xPt_3O_4$ was prepared according to Cahen's method[21] using 2 $CdCO_3$ and 1 $(NH_4)_2PtCl_6$ at 575 °C under flowing O_2. After treatment with aqua regia, the product was $Cd_{0.40}Pt_3O_4$ (Cd = 6.55%, a = 5.6673 Å).

The fluoride–nitrate reaction results in a mixture of $M_xPt_3O_4$, $CdPt_3O_6$, and Cd_2PtO_4. The reaction of 1 $Cd(NO_3)_2 \cdot 4H_2O$ and 3 PtO_2 produced an $M_xPt_3O_4$ phase and a minor amount of an unidentified phase. The majority phase was analyzed to be 3.51% Cd and 1.50% Na, corresponding to $\sim Cd_{0.29}Na_{0.44}Pt_3O_4$. Hydrothermal reactions using CdO, PtO_2, and NH_4OH at 700 °C and 2000 atm produced either $CdPt_3O_6$ or mixtures of $Cd_xPt_3O_4$, $CdPt_3O_6$, and PtO_2.

$H_xPt_3O_{4-y}Cl_y$. Heating H_2PtCl_6 in HNO_3 vapor at up to 425 °C yielded only $PtCl_2$ as a crystalline phase; increasing the temperature to 440 °C gave mainly PtO_2 with traces of Pt metal. However, when steam was used at 425–450 °C, the product was a high-surface-area bronze (up to 76 m^2/g) plus Pt. Removal of the Pt with aqua regia gave yields of pure bronze of 40–60%, based on *initial* platinum content. A high-temperature Guinier study indicates decomposition to Pt at 545–560 °C; the line width is great enough to preclude an accurate determination of the cubic cell dimension, but a is approximately 5.76 Å. Boiling the "bronze" for extended periods with nitric acid does not change the X-ray pattern but does result in very slow dissolution.

After the sample was dried at 200 °C under vacuum, H, O, and Cl analyses indicated 0.05, 8.45, and 4.6%, respectively, and did not correspond to $H_xPt_3O_4$. TGA of a sample before it was heated to 200 °C showed 1% weight loss after 2 h at 200 °C under vacuum and 13.1% between 400 and 600 °C with ~12% weight loss occurring between 500 and 600 °C. If we assume that the 1% weight loss at 200 °C corresponds to adsorbed H_2O, we arrive at the composition $H_{0.3}Pt_3O_{3.25}Cl_{0.75}$. The Cl substitution for O is consistent with the unusually large cell dimension.

Attempts to prepare transition-metal bronzes $M_xPt_3O_4$ (M = V, Fe, Cr, Mn, etc.) analogous to the known $Li_xPt_3O_4$ and $Ni_xPt_3O_4$ were not successful, but some of these metals can be incorporated at a low level, probably via a doping mechanism. For example, if an equiatomic mixture of platinum and vanadium (as the pentoxide) is dissolved in aqua regia and the solids from the resulting dried solution are treated with steam at 460 °C for 4 h, a product containing V_2O_5, Pt, and a bronze phase is recovered. Treatment with warm aqua regia removes all phases but the bronze, which is produced in 40–60% yield. The surface area is about 40 m^2/g, and the analysis corresponds to $V_{0.1}Pt_3O_2(OH)_2$, on the basis of results for O, H, and V. The X-ray diffraction pattern consists of broad lines (a = 5.66 Å), similar to that of the undoped material. If HNO_3 is used as the hydrolysis gas, the products are V_2O_5 and Pt, even at 450 °C.

In a similar way, if an equiatomic mixture of Fe–Pt is converted to the chlorides and hydrolyzed at 425 °C with steam, the product is an iron-containing bronze after removal of Fe_2O_3 and platinum in aqua regia. The yield is rather low (30%), and the product contains 1.0% Fe, corresponding probably to $Fe_{0.12}Pt_3O_{4-y}Cl_y$. The surface area is 32 m^2/g, and the cubic X-ray pattern (broad lines) is satisfactorily indexed with a = 5.73 Å.

A chromium-doped bronze of uncertain composition was prepared in about 60% yield from chromium and platinum chlorides (Cr/Pt = 0.3). The surface area was 49 m^2/g, and the cell edge a = 5.75 Å.

Miscellaneous Syntheses. Attempts to prepare $M_xPt_3O_4$ phases using hydrothermal, nitrate, fluoride–nitrate, or carbonate reactions were unsuccessful for M = Al, Ti, V, Cr, Fe, Y, Zr, Nb, Ta, Rh, In, Sn, La, Ce, Bi, and Hg.

$Cu(NO_3)_2 \cdot 3H_2O$ and 3 PtO_2 react to give a mixture of $M_xPt_3O_4$ and $Cu_{1-x}Pt_xO$.[40] Because of the presence of two phases insoluble in aqua regia, the $M_xPt_3O_4$ phase could not be analyzed. We suspect M is primarily Na. Two-phase mixtures also resulted when attempts were made to prepare $Tl_xPt_3O_4$, $Th_xPt_3O_4$, $Pb_xPt_3O_4$, and $Mn_xPt_3O_4$. It was thus not possible to confirm the existence of these phases.

Results and Discussion

High-Temperature Guinier Studies. Because of the confusion over results obtained by various investigators on reaction products, a number of reactions resulting in $M_xPt_3O_4$ were studied by high-temperature X-ray diffraction. Although these reactions do not reproduce exactly the LS experiments run over 400 h, they represent the best information we have available.

(39) Lyman, C. E., personal communication.

(40) Muller, O.; Roy, R. *J. Less-Common Met.* **1969**, *19*, 209.

Table II. High-Temperature Study of $M_xPt_3O_4$ Reactions

M	reacn no.	reacn
Li	1	$LiNO_3 + 3\alpha\text{-}PtO_2 \xrightarrow[\text{air}]{600\ ^\circ C} Li_xPt_3O_4 + Pt \xrightarrow{760\ ^\circ C} Li_2PtO_3 + Pt$
	2	$LiF + LiNO_3 + 6\alpha\text{-}PtO_2 \xrightarrow[\text{air}]{575\ ^\circ C} Li_xPt_3O_4 + Pt \xrightarrow{700\ ^\circ C} Li_2PtO_3 + Pt \xrightarrow{920\ ^\circ C} Pt$
	3	$LiF + LiNO_3 + 6\alpha\text{-}PtO_2 \xrightarrow[\text{He}]{465\ ^\circ C} Li_2PtO_3 + Pt \xrightarrow{700\ ^\circ C} Pt$
Ca	4	$Ca(NO_3)_2\cdot 4H_2O + 3\alpha\text{-}PtO_2 \xrightarrow[\text{air}]{650\ ^\circ C} CaPt_3O_4 \xrightarrow{700\ ^\circ C} CaPt_2O_4 + Pt \xrightarrow{950\ ^\circ C} Ca_4PtO_6 + Pt$
	5	$2CaCO_3 + (NH_4)_2PtCl_6 \xrightarrow[\text{air}]{300\ ^\circ C} \text{unident I} \xrightarrow{375\ ^\circ C} \text{unident II} \xrightarrow{650\ ^\circ C} CaPt_2O_4 \xrightarrow{850\text{-}900\ ^\circ C} Ca_4PtO_6 + Pt$
Cd	6	$2CdCO_3 + (NH_4)_2PtCl_6 \xrightarrow[O_2]{265\ ^\circ C} CdCl_2 \xrightarrow{440\ ^\circ C} \text{amorphous} \xrightarrow{600\ ^\circ C} CdPt_3O_6 \xrightarrow[O_2]{800\ ^\circ C} Cd_2PtO_4$
	7	$2CdCO_3 + (NH_4)_2PtCl_6 \xrightarrow[\text{air}]{250\ ^\circ C} CdCl_2 \xrightarrow{350\ ^\circ C} CdO + Pt \xrightarrow{600\ ^\circ C} Cd_2PtO_4 + \text{unident} \xrightarrow{840\ ^\circ C} CdO + Pt$
Co	8	$CoF_2 + \alpha\text{-}PtO_2 \xrightarrow[\text{air}]{190\ ^\circ C} \alpha\text{-}PtO_2 + Co_3O_4 \xrightarrow{650\ ^\circ C} PtCoO_2 + Pt + Co_3O_4 \xrightarrow{800\ ^\circ C} Pt + Co_3O_4 \xrightarrow{925\ ^\circ C} Pt + CoO$
	9	$CoCO_3 + 3\alpha\text{-}PtO_2 \xrightarrow[\text{He}]{380\ ^\circ C} Co_3O_4 + PtO_2 \xrightarrow{450\ ^\circ C} Pt + Co_3O_4 \xrightarrow{725\ ^\circ C} Pt + CoO$
	10	$0.25LiF + 0.75Co(NO_3)_2\cdot 6H_2O + 3\alpha\text{-}PtO_2 \xrightarrow[\text{air}]{650\ ^\circ C} Co_xLi_yPt_3O_4 + Pt \xrightarrow{675\ ^\circ C} PtCoO_2 + Co_xLi_yPt_3O_4 + Pt \xrightarrow{760\ ^\circ C} PtCoO_2 + Pt \xrightarrow{800\ ^\circ C} Pt + Co_3O_4(?)$
	11	$0.25LiF + 0.75Co(NO_3)_2\cdot 6H_2O + 3\alpha\text{-}PtO_2 \xrightarrow[\text{He}]{525\ ^\circ C} Pt$
Ni	12	$NaF + NiF_2 + 6\alpha\text{-}PtO_2 \xrightarrow[\text{air}]{625\ ^\circ C} Ni_xNa_yPt_3O_4 + Pt \xrightarrow{790\ ^\circ C} Pt + NiO$
	13	$NaF + NiF_2 + 6\alpha\text{-}PtO_2 \xrightarrow[\text{He}]{435\ ^\circ C} Pt + NiO$
	14	$Ni(NO_3)_2\cdot 6H_2O + 3\alpha\text{-}PtO_2 \xrightarrow[\text{air}]{650\ ^\circ C} Ni_xNa_yPt_3O_4 + Pt \xrightarrow{775\ ^\circ C} Pt + NiO$
	15	$NaF + Ni(NO_3)_2\cdot 6H_2O_5 + \alpha\text{-}PtO_2 \xrightarrow[\text{He}]{525\ ^\circ C} Pt + NiO$

Reactions run to prepare $M_xPt_3O_4$ with M = Li, Ca, Cd, Co, and Ni are summarized in Table II. Only the phases detected by X-rays are included; thus, amorphous phases and those present in <5% quantity are not detected. As noted in BK,[22] reaction 1 between $LiNO_3$ and PtO_2 produces $Li_xPt_3O_4$ with Pt impurity. The reaction occurs just as PtO_2 decomposes at ~575–600 °C. $Li_xPt_3O_4$ further disproportionates into Li_2PtO_3 and Pt at 760 °C as noted by LS. A reaction involving LiF and $LiNO_3$ is similar, but the product $Li_xPt_3O_4$ disproportionates at 700 °C. Because LS[23,24] reported successful synthesis in an inert atmosphere, we performed several HTG's in He. In the case of reaction 3, the decomposition of PtO_2 begins much earlier but we find no $Li_xPt_3O_4$.

Reaction 4 between calcium nitrate and PtO_2 produces $CaPt_3O_4$ as noted in BK. $CaPt_3O_4$ has a stability region of only 50 °C; above 700 °C it decomposes to $CaPt_2O_4$ + Pt. Interestingly reaction 5, as noted by CIW,[21] does not produce $CaPt_3O_4$ but only $CaPt_2O_4$. CIW searched for an explanation for the lack of stability of $Ca_xPt_2O_4$; the answer appears to lie in the extreme dependence of these reactions on the nature of the reagents.

Reaction 6 between $CdCO_3$ and $(NH_4)_2PtCl_6$ under flowing O_2 is the reaction used by CIW to produce $Cd_xPt_3O_4$ and $CdPt_3O_6$. It is interesting that this reaction proceeds via $CdCl_2$ formed from $CdCO_3$ and $(NH_4)_2PtCl_6$ and even through an amorphous phase. The development of $CdPt_3O_6$ from this amorphous phase is presumably what leads to a high-surface-area product (30 m^2/g). Reaction 7 run in air produces $CdCl_2$ and then CdO and Pt, which further react to form Cd_2PtO_4.

The reaction of CoF_2 with PtO_2 in air proceeds via Co_3O_4 to $PtCoO_2$ + Pt and Co_3O_4. This procedure followed by an aqua regia treatment to dissolve Pt and Co_3O_4 is a simpler method of preparing $PtCoO_2$ than reported earlier.[37,41] The same reaction run in He produces only Pt and Co_3O_4.

Reactions 2 and 10 represent the high-yield fluoride–nitrate reactions for synthesis of $M_xPt_3O_4$. They, along with reactions 1, 4, 12, and 14, show that the reaction to form $M_xPt_3O_4$ occurs at the temperature where PtO_2 decomposes. Running the reaction at a lower P_{O_2}, although it causes the decomposition to occur at a lower temperature (435 → 525 °C), does not allow formation of $M_xPt_3O_4$. Apparently the reactivity of NiO or Co_3O_4 is too low at 400–500 °C. These results are not in accord with the results of LS, who claim synthesis of these oxides in Ar. However, it should be noted that the HTG results are obtained over a period of 24 h whereas the LS results were obtained after 400 h.

The high-temperature X-ray results point out the unusual dependence of $M_xPt_3O_4$ products on specific reagents. This is certainly the cause of CIW's inability to prepare $Ca_xPt_3O_4$ and may be responsible for other discrepancies in various investigators' work, e.g., our inability to prepare $Cu_xPt_3O_4$ and $Ag_xPt_3O_4$ reported by Thiele et al.[2] and LS. However, in the case of $K_xPt_3O_4$ and $Ba_xPt_3O_4$ the existence of these compounds is doubtful from unit cell dimensions (see below).

Chemical and X-ray Analysis. The cell dimensions of many of the compounds prepared are listed in Table I. Cell di-

(41) Shannon, R. D. U.S. Patent 3 514 414, 1970; U.S. Patent 3 629 156, 1971.

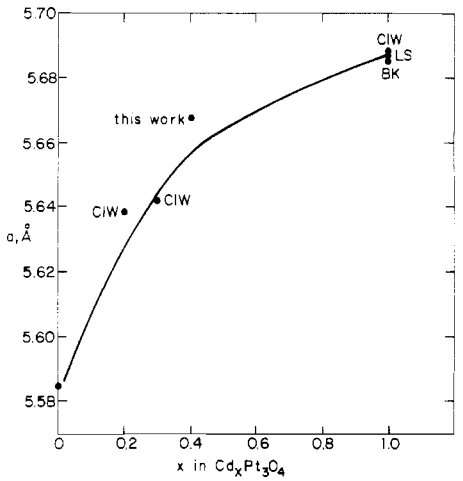

Figure 1. Cell dimensions of $Cd_xPt_3O_4$ vs. x.

mensions of the samples prepared by vapor-phase hydrolysis are omitted because of the inaccurate "d" values obtained from the broad X-ray lines. The only samples with x approaching 1 were $NaPt_3O_4$ and $CaPt_3O_4$. Although CIW were able to prepare $CdPt_3O_4$, our analysis of a similar reaction resulted in $Cd_{0.4}Pt_3O_4$. Most of the reactions produced $M_xNa_yPt_3O_4$ solid solutions with $x + y$ ranging from 0.4 to 0.8. We were not able to prepare the Co or Ni varieties with $x > 0.5$.

The Na and Cd compositions appear to have variable compositions with cell dimensions dependent on x as noted by CIW. There are only a few samples whose compositions are well enough known to determine this relationship. A linear relationship between x and a was found for $Na_xPt_3O_4$.[16] The same plot for $Cd_xPt_3O_4$ appears to be parabolic (Figure 1).

Most compositions readily accept Na in solid solution. On the basis of cell dimensions we believe that compositions prepared by both LS and BK containing Mg, Ni, Co, and Zn had a significant Na content and that the compositions containing K and Ba were, in fact, $Na_xPt_3O_4$. Compositions containing the smaller divalent cations Mg and Zn and the transition-metal cations Co and Ni appear to readily accept larger cations such as Na. Indeed, cation size seems to influence the value of x: only the larger cations Na, Cd, and Ca seem to allow $x = 1$. The maximum value we found for Li was 0.8. Smaller values such as 0.5 seem to be the rule for Co and Ni.

These composition limits seem to be associated with structural deformations of the $NaPt_3O_4$ structure.[42] In $Li_{0.64}Pt_3O_4$ movement of the O atoms away from the special position $^1/_4$, $^1/_4$, $^1/_4$ lowers the space-group symmetry from $Pm3n$ to $P43n$ and causes the eight-coordinated Li–O polyhedron to distort from a cube to an eight-coordinated polyhedron consisting of two interpenetrating tetrahedra with Li–O distances of 2.221 and 2.649 Å. In $Co_{0.37}Na_{0.14}Pt_3O_4$ ordering of Co and Na cations into sites at 0, 0, 0 and vacancies into sites at $^1/_2$, $^1/_2$, $^1/_2$ reduce the space-group symmetry from $Pm3n$ to $Pm3$. The oxygen atoms surrounding the cation site at 0, 0, 0 move toward this site to give an average (Co,Na)–O distance of 2.36 Å and away from the vacant site to give a vacancy–oxygen distance of 2.52 Å. In both cases the structure has distorted to allow the more chemically reasonable crystal interatomic distances associated with the small ions Li^+ and Co^{2+}. The observation of an empirical x_{max} of 0.5 for small cations Mg^{2+}, Zn^{2+}, Co^{2+}, and Ni^{2+} is accounted for by the structural distortions. Although the structures of $Zn_xPt_3O_4$ and $Mg_xPt_3O_4$ were not determined, similar structural distortions should be anticipated.

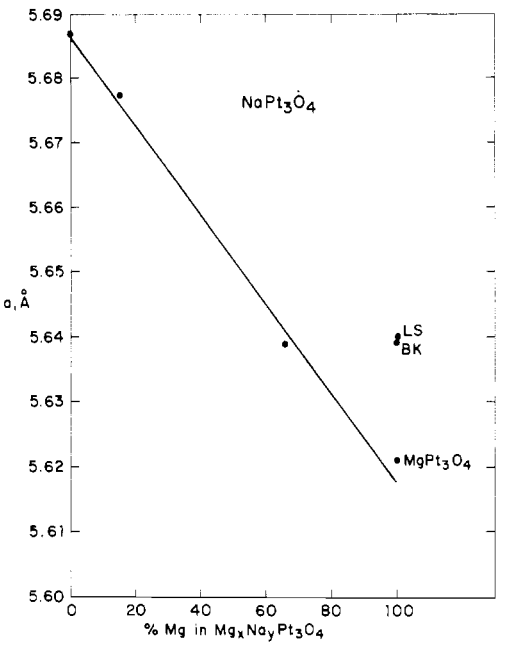

Figure 2. Cell dimensions of $Mg_xNa_yPt_3O_4$ vs. % Mg.

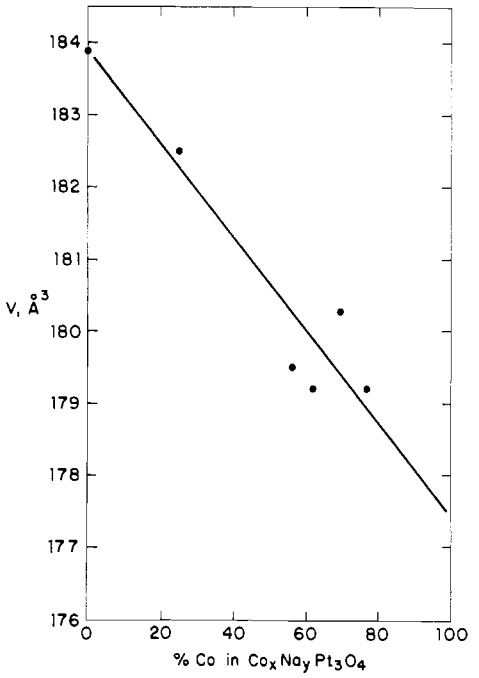

Figure 3. Cell dimensions of $Co_xNa_yPt_3O_4$ vs. % Co.

Both Sukhotin et al.[43] and CIW commented on the deficiency of oxygen in $Na_xPt_3O_4$ compositions and suggested the presence of Pt interstitials, O vacancies, or impurity ions on oxygen sites. In Table I are listed oxygen analyses for $Li_xPt_3O_4$, $NaPt_3O_4$, $Co_xNa_yPt_3O_4$, and $Ni_xNa_yPt_3O_4$. The Na and Co–Na compositions show considerable O deficiency whereas the Li and Ni–Na compositions show reasonable agreement between observed and calculated oxygen content. However, because the neutron diffraction refinement of the structure of $NaPt_3O_4$[16] shows no apparent oxygen vacancies or Pt interstitials, the oxygen deficiencies in Table I and those measured by CIW and Sukhotin et al.[42] are probably in error.

(42) Schwartz, K. B.; Parise, J. B.; Prewitt, C. T.; Shannon, R. D. *Acta Crystallogr.*, in press.

(43) Sukhotin, A. M.; Gankin, E. A.; Kondrashov, Y. D.; Omelchenko, Y. A.; Shalman, B. Y. *Russ. J. Inorg. Chem.* (*Engl. Transl.*) **1971**, *16*, 1690.

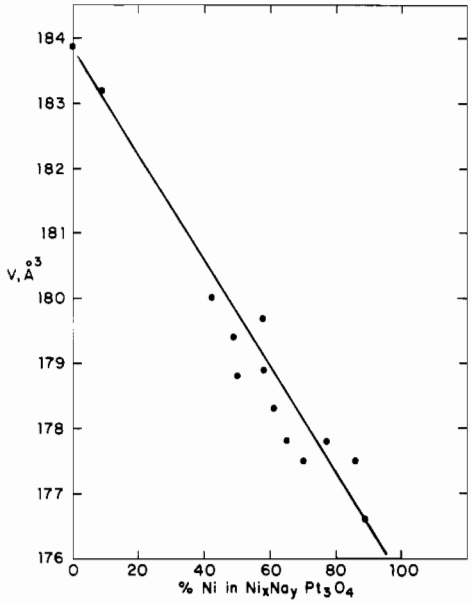

Figure 4. Cell dimensions of $Ni_xNa_yPt_3O_4$ vs. % Ni.

We do not have an explanation for these apparent oxygen deficiencies, but perhaps they can be attributed to the presence of an amorphous second phase with a lower oxygen content or to the presence of a form of Pt which will not give up all its oxygen during analysis.

It would be convenient to make plots of a vs. % M, but this is complicated by the dependence of a on x (see Figure 1). Nevertheless, we have attempted these plots for the compositions $Mg_xNa_yPt_3O_4$, $Co_xNa_yPt_3O_4$, and $Ni_xNa_yPt_3O_4$ (Figures 2–4) and find them approximately linear. This linear fit is excellent considering the dependence of a on total cation content, $x + y$. Although x was not given for $Mg_xPt_3O_4$ by Muller and Roy, it would seem from this plot and Table I that the Muller and Roy sample could be $Mg_{0.5}Pt_3O_4$.

Figures 3 and 4 show similar plots for $Co_xNa_yPt_3O_4$ and $Ni_xNa_yPt_3O_4$. Again we see an approximately linear dependence of unit cell volume on % Co or % Ni content. The scatter may be the result of the dependence of a on $x + y$. The Co plot extrapolates to $a \simeq 5.62$ Å for pure $Co_xPt_3O_4$, and from Table I we surmise x in pure $Co_xPt_3O_4$ is about 0.5. Similarly we estimate $a(Ni_xPt_3O_4) \simeq 5.60$ and $x_{max} \simeq 0.5$. The cell dimensions are reasonably consistent with ionic radii: $r(Mg^{2+}) = 0.72$, $r(Co^{2+}) = 0.745$, and $r(Ni^{2+}) = 0.69$ Å.

XPS. The E_B values for the Pt $4f_{7/2}$ photoelectron were determined for approximately 30 $M_xPt_3O_4$ compositions and are listed in Table III. The average value of 72.4 ± 0.2 eV is in agreement with values for square-planar Pt(II) obtained by Cahen et al.[21] for $NaPt_3O_4$, $Cd_xPt_3O_4$, $CaPt_2O_4$, and $CdPt_3O_6$ and can be compared to 71.2 eV for metallic Pt,[44,45] 72.4 eV for PtO,[45-47] 71.9 eV for Pt^+ in $PtCoO_2$,[21] and 74.4 eV for PtO_2.[21,46,47] Metallic character of the platinum appears to have little effect since the E_B's of Pt in metallic $M_xPt_3O_4$ are the same as in semiconducting PtO.

The O 1s peak is broad and has a high-energy shoulder. The two peaks can be deconvoluted to give peaks at approximately 530.6 and 532.3 eV with intensity ratios of 3/1 to 5/1. The intensities of the 532-eV tail diminished by about 25% in samples heated at 200 °C under vacuum. These high-energy tails were also noted by Hecq et al.[45] in sputtered PtO_2 and PtO_{1+x} and were ascribed to adsorbed oxygen and/or chemisorbed oxygen species. A similar phenomenon was observed in $Li_xNi_{1-x}O$ by Sugano et al.,[48] in CoO, Co_3O_4, Fe_2O_3, and ZnO by Haber et al.,[49] in the oxidation of Ni by Allen et al.,[50] and in CoO and Co_3O_4 by Chuang et al.[51] Allen et al.[50] observed a strong peak at 529.9 eV, attributable to oxygen atoms that are part of the NiO lattice, and a shoulder at 531.6 eV with an intensity ratio $I_{529.9}/I_{531.6} \simeq 2.2/1$. The shoulder was attributed to an adsorbed or chemisorbed oxygen species. It was necessary to heat the oxide to 275–300 °C to remove the adsorbed O_2 completely. A similar doublet was found in an XPS study of IrO_2 films.[52] The high-energy tail was attributed to adsorbed H_2O.

Efforts were also made to identify and characterize the Co 2p and Ni 2p photoelectron spectra in the cobalt and nickel platinum oxides. In many samples these spectra were too weak to detect, indicating either surface depletion or surface overlayer effects. In the $Co_xNa_yPt_3O_4$ compositions, E_B of the Co $2p_{3/2}$ peak varied from 780.2 to 780.9 eV (see Table III). The values were obtained on spectra with low signal/noise ratios, and thus the precision of the E_B measurement is poor. Although McIntyre and Cook[53] claim that changes in formal oxidation state do not result in a change in the E_B value of the Co 2p lines, Chuang et al.[51] state that, with careful measurements of the Co 2p spectra, it is possible to distinguish between CoO and Co_3O_4. They observed E_B values of 780.5

Table III. XPS Data

compd	binding energies, eV: Pt $4f_{7/2}$	O 1s	A	atomic ratios, M/Pt: M	XPS	chem anal.
$Li_{0.63}Pt_3O_4$	72.1	530.6	*a*	Li		0.22
$Li_{0.80}Pt_3O_4$	72.0	530.6	*a*	Li		0.27
$Na_{0.22}Pt_3O_4$	72.7	530.6	1072.4[b]	Na	0.05	0.07
$Na_{1.0}Pt_3O_4$	72.1	530.6	1072.1[b]	Na	0.40	0.33
$Cd_{0.40}Pt_3O_4$	72.6	530.6	405.3[c]	Cd	0.35	0.15
$Co_{0.21}Na_{0.61}Pt_3O_4$	72.4	530.6	780.6[d]	Co	0.02	0.07
			1072.3[b]	Na	0.18	0.20
$Co_{0.38}Na_{0.38}Pt_3O_4$	72.4	530.6	780.6[d]	Co	0.11	0.13
			1072.4[b]	Na	0.17	0.13
$Co_{0.50}Na_{0.15}Pt_3O_4$	72.4	530.6	780.2[d]	Co	0.11	0.17
			1072.2[b]	Na	0.03	0.05
$Co_{0.61}Na_{0.28}Pt_3O_4$	72.3	530.6	780.2[d]	Co	0.10	0.20
			1072.1[b]	Na	0.10	0.09
$Ni_{0.38}Na_{0.38}Pt_3O_4$	72.4	530.6		Ni	tr[f]	0.13
			1072.4[b]	Na	0.15	0.13
$Ni_{0.47}Na_{0.34}Pt_3O_4$	72.4	530.6	tr[f]	Ni	tr	0.16
			1072.5[b]	Na	0.16	0.11
$Ni_{0.52}Na_{0.12}Pt_3O_4$	72.4	530.6	855.9[e]	Ni	0.06	0.17
			1072.2[b]	Na	0.01	0.04
$Ni_{0.53}Na_{0.08}Pt_3O_4$	72.5	530.6	854.8[e]	Ni	0.20	0.18
			1072.3[b]	Na	0.02	0.03
$Ni_{0.34}Pt_3O_4$	72.6	530.6	854.9[e]	Ni	0.09	0.11
$Ni_{0.35}Pt_3O_4$	72.5	530.6	855.7[e]	Ni	0.13	0.11
$Ni_{0.42}Pt_3O_4$	72.6	530.6	855.6[e]	Ni	0.13	0.14
$Ni_{0.48}Pt_3O_4$	72.5	530.6	855.1[e]	Ni	0.06	0.16

[a] No data on lithium, since the single lithium photoelectron peak, Li 1s, occurs in the same energy range as the Pt 5p photoelectrons. [b] A = Na 1s. [c] A = Cd $3d_{5/2}$. [d] A = Co $2p_{3/2}$. [e] A = Ni $2p_{3/2}$. [f] tr = trace detected.

(44) Baer, Y.; Heden, P. F.; Hedman, J.; Klasson, M.; Nordling, C.; Siegbahn, K. *Phys. Ser. 1* **1970**, *55*.
(45) Hecq, M.; Hecq, A.; Delrue, J. P.; Robert, T. *J. Less-Common Met.* **1979**, *64*, 25.
(46) Bancroft, G. M.; Adams, I.; Coatsworth, L. L.; Bennewitz, C. D.; Brown, J. D.; Westwood, W. D. *Anal. Chem.* **1975**, *47*, 586.
(47) Kim, K. S.; Winograd, N.; Davis, R. E. *J. Am. Chem. Soc.* **1971**, *93*, 6296.
(48) Sugano, T.; Ohta, T.; Kuroda, H. *Proc. Int. Conf. Solid Surf., 2nd* **1974**; *J. Appl. Phys., Suppl. 2* **1974**, 799 (Part 2).
(49) Haber, J.; Stoch, J.; Ungier, L. *J. Electron Spectrosc. Relat. Phenom.* **1976**, *9*, 459.
(50) Allen, G. C.; Tucker, P. M.; Wild, R. K. *Oxid. Met.* **1979**, *13*, 223.
(51) Chuang, T. J.; Brundle, C. R.; Rice, D. W. *Surf. Sci.* **1976**, *59*, 413.
(52) Kim, K. S.; Sell, C. D.; Winograd, N. *Proc. Symp. Electrocatal.* **1974**.
(53) McIntyre, N. S.; Cook, M. G. *Anal. Chem.* **1975**, *47*, 2208.

Table IV. Magnetic Susceptibilities of $M_xPt_3O_4$

sample	fw	A, emu/g	C, emu K/g	Θ, K	C_M, emu/mol	η^*_{eff}, μ_B	comments
$NaPt_3O_4$	672.3	$\chi_{RT} = 0.86 \times 10^{-6}$ emu/g					*a*
$Li_{0.80}Pt_3O_4$	654.7	$\chi_{RT} = 0.22 \times 10^{-6}$ emu/g					
$Li_{0.75}Na_{0.14}Pt_3O_4$	657.7	$\chi_{RT} = 0.060 \times 10^{-6}$ emu/g					
$Li_{0.76}Pt_3O_4$	654.5	$\chi_{RT} = 0.043 \times 10^{-6}$ emu/g					
$Co_{0.50}Na_{0.15}Pt_3O_4$	682.2	0.300×10^{-6}	0.154×10^{-2}	−41	1.051	4.10	cubic
$Ni_{0.36}Pt_3O_4$	670.4	0.401×10^{-6}	0.403×10^{-3}	−0.9	0.267	2.88	
$Ni_{0.47}Na_{0.34}Pt_3O_4$	684.7	0.905×10^{-6}	0.445×10^{-3}	10	0.305	2.35	cubic
$Ni_{0.48}Pt_3O_4$	677.5	0.146×10^{-6}	0.557×10^{-3}	−17	0.377	2.56	
$Ni_{0.52}Na_{0.12}Pt_3O_4$	682.6	0.118×10^{-6}	0.684×10^{-3}	5.6	0.467	2.63	noncubic
$Ni_{0.53}Na_{0.08}Pt_3O_4$	682.3	0.367×10^{-6}	0.682×10^{-3}	47	0.465	2.57	noncubic
Ni^{3+}						3.87[b] (4.0[c])	
Ni^{2+}						2.83[b] (2.9–3.5[c])	
Co^{3+}						4.90[b] (5.3[c])	
Co^{2+}						3.87[b] (4.0[c])	

[a] Not Curie–Weiss behavior. [b] Spin-only moments. [c] Typical values in the complexes are from: Figgis, B. N.; Lewis, J. *Prog. Inorg. Chem.* **1964**, 6, 37.

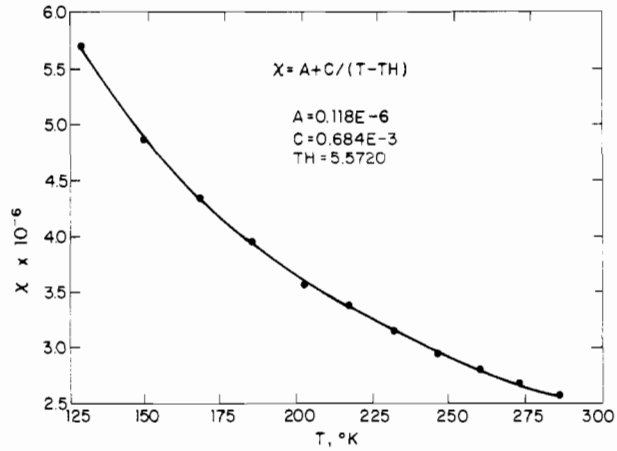

Figure 5. χ vs. T for $Ni_{0.52}Na_{0.12}Pt_3O_4$.

eV for Co^{2+} and 779.6 eV for Co^{3+}. Because of the poor quality of the Co 2p spectra (low intensity, low S/N), it is difficult to make an unambiguous assignment of the oxidation state of cobalt, but the E_B values suggest the presence of Co^{2+}.

In the $Ni_xNa_yPt_3O_4$ compositions, the E_B values of the Ni $2p_{3/2}$ peaks were in the range 854.7–856.1 eV. Here, as with the cobalt platinum oxides, many of the transition-metal spectra were of poor quality. The Ni $2p_{3/2}$ spectra were similar to those found in NiO and $NiFe_2O_4$ with the photoelectron peak at ~855 eV and the shake-up satellite at ~862 eV.[53,54] Thus we conclude that nickel is probably divalent.

Magnetic Susceptibility. Magnetic susceptibility data were fitted to the expression $\chi = A + C/(T - \Theta)$, where A represents the Pauli paramagnetic contribution and C the localized moment contribution. Θ is the Weiss constant (see Figure 5). The results are summarized in Table IV where C_M is the molar Curie constant and η^*_{eff} is the magnetic moment per transition-metal ion, M.

In $Na_xPt_3O_4$ and $Li_xPt_3O_4$ Na and Li should not have localized moments in this structure, so that the measured susceptibility should be the sum of the essentially temperature-independent diamagnetic core and paramagnetic conduction electron contribution plus any paramagnetic impurity contribution. $NaPt_3O_4$ is Pauli paramagnetic with a room temperature value of χ of 0.86×10^{-6} emu/g; this is close to the value given by CIW of 0.55×10^{-6} emu/g. The susceptibility of $Li_xPt_3O_4$, which might be expected to be similar to that of $NaPt_3O_4$, actually shows Curie–Weiss behavior with values of $(0.04–0.22) \times 10^{-6}$ emu/g. An independent determination of the room-temperature susceptibility by NMR gave $(0.20 \pm 0.5) \times 10^{-6}$ emu/g. From Tables IV and V we see that the susceptibility of $Li_xPt_3O_4$ is proportional to the total number of paramagnetic impurities (~0.01–0.2%). In fact, recent susceptibility measurements on a purer sample of $Li_xPt_3O_4$ made from the CLAL PtO_2 show it to be diamagnetic.[55] We do not understand the differences in χ in $Li_xPt_3O_4$ and $NaPt_3O_4$, but it probably is related to the nonstoichiometry in the M site and/or to the structural distortion observed in $Li_xPt_3O_4$.

Table V. Emission Spectrographic Analyses (Ppm) of $NaPt_3O_4$ and $Li_xPt_3O_4$

	$NaPt_3O_4$	$Li_{0.8}Pt_3O_4$	$Li_{0.75}Na_{0.14}Pt_3O_4$	$Li_{0.76}Pt_3O_4$
Na		500–2500		
Mg	10–50	100–500	10–50	10–50
Ca	50–250	500–2500	50–250	50–250
Ba	500–2500	500–2500		
B		5–25	20–100	
Al		200–1000	5–25	5–25
Si		50–250	20–100	20–100
Cr		20–100		20–100
Mn		50–250	10–50	10–50
Fe	10–50	200–1000	5–25	5–25
Co				
Ni		200–1000	50–250	10–50
Cu	20–100	50–250	2–10	2–10
Ag	2–10			
Sn		50–250		
Pb		20–100	20–100	20–100
Pd			20–100	2–10

The susceptibilities of $Co_{0.50}Na_{0.15}Pt_3O_4$ and the $Ni_xNa_yPt_3O_4$ compounds are best fitted with the sum of a temperature-independent term plus a Curie–Weiss term, the former being 5–10% of the latter at 300 K. Presumably, the temperature-independent part is the result of electronic conduction through the short Pt–Pt bonds; the Ni (or Co) may or may not contribute, depending upon location in the lattice. The temperature-dependent susceptibilities fit well to Curie–Weiss plots with relatively small Weiss constants, allowing effective moments to be calculated.

The effective moment of Co in $Co_{0.50}Na_{0.15}Pt_3O_4$, 4.10 μ_B, is close to the value of 4.60 μ_B for 8-coordinated Co^{2+} in $[As(C_6H_5)_4]_2[Co(NO_3)_4]$.[56,57] In an independent measurement by Schwartz et al.[55] on $Co_{0.37}Na_{0.14}Pt_3O_4$, a value of 3.64 μ_B was obtained. We believe that these data in conjunction with the XPS data confirm the presence of Co^{2+} in the $M_xPt_3O_4$ compositions.

(54) Allen, G. C.; Tucker, P. M.; Wild, R. K. *Proc. Int. Vac. Congr., 7th* **1977**, 959.
(55) Schwartz, K. B.; Parise, J. B., to be submitted for publication.
(56) Bergman, J. G.; Cotton, F. A. *Inorg. Chem.* **1966**, *5*, 1208.
(57) Cotton, F. A.; Bergman, J. G. *J. Am. Chem. Soc.* **1964**, *86*, 2941.

The moments (2.35–2.57 μ_B) observed for Ni in the four $Ni_xNa_yPt_3O_4$ compositions listed in Table IV are typical for Ni^{2+} compounds.

Electrical Conductivity. CIW found that $CaPt_2O_4$, $Cd_xPt_3O_4$, and $Na_xPt_3O_4$ powders exhibit metallic conductivity. This was consistent with the single-crystal resistivity measurements in $Ni_{0.25}Pt_3O_4$.[18] However, semiconducting behavior was reported for $Cu_{0.5}Pt_3O_4$, $Mg_{0.7}Pt_3O_4$, $MgPt_3O_4$, $ZnPt_3O_4$, $CaPt_3O_4$, and $BaPt_3O_4$.[23,24]

We have measured the conductivity of $NaPt_3O_4$ crystals[16] and polycrystalline $Li_xPt_3O_4$. The $Na_xPt_3O_4$ crystals have typical metallic resistivity with $\rho(RT) = 9 \times 10^{-5}$ Ω cm, slightly higher than that of $Ni_{0.25}Pt_3O_4$ ($\rho(RT) = 3 \times 10^{-5}$ Ω cm). The $Li_xPt_3O_4$ sintered bar has a much higher resistivity ($\rho(RT) = 1.1 \times 10^{-4}$ Ω cm) with only a small positive temperature dependence ($\rho(50\,K) = 0.8 \times 10^{-4}$ Ω cm). The higher resistivity of this sample perhaps results from grain boundary effects, but in light of the unique structural distortions and the diamagnetic susceptibility of $Li_xPt_3O_4$, we believe $Li_xPt_3O_4$ may be a semimetal.

These conductivity results in conjunction with those on $Ni_{0.25}Pt_3O_4$ and the powder specimens of CIW along with the short Pt–Pt bonds are sufficient evidence to conclude that most compounds with the $M_xPt_3O_4$ structure have metallic conductivity. The semiconductor behavior observed by Lazarev and Shaplygin[23,24] may be caused by the presence of an insulating second phase, perhaps α-PtO_2. Their further generalization that all double oxides containing metals with a d^6 or d^8 configuration (Pt(II,IV)) are semiconductors is clearly not valid.

Because of the claim that $NaPt_3O_4$ exhibited ionic conductivity,[14] we tried to exchange Na for Li by heating a sample in excess $LiNO_3$ at 300 °C for 24 h. Because only 14 ppm Li was found in the $NaPt_3O_4$ sample after this treatment, we conclude that at least the Na form of $M_xPt_3O_4$ is probably not an ionic conductor. This is consistent with the lack of continuous channels connecting Na ions in the $NaPt_3O_4$ structure.

NMR of $H_xPt_3O_{4-y}Cl_y$. It was found by NMR that an untreated sample contained 0.17% hydrogen. Chemical analysis of the same sample showed 4.6% Cl. This corresponds to an atomic ratio of H/Cl of 1.1:0.8. After the sample was heated for 16 h at 200 °C under high vacuum, the H and Cl contents dropped to 0.05% H and 4.4% Cl, corresponding to $H_{0.3}Pt_3O_{3.25}Cl_{0.8}$. The line width of the untreated sample at room temperature was 0.6 kHz, which is considerably less than the 8.4-kHz width of the heat-treated sample. This indicates that the hydrogen driven off by the heat treatment was present as a highly mobile species, probably surface-adsorbed H_2O, and the composition of starting material was $H_{0.3}Pt_3O_{3.25}Cl_{0.75}\cdot 1.2H_2O$ (adsorbed).

The hydrogen species in the heat-treated sample is much less mobile. Its NMR spectrum broadens from 8.4 kHz at room temperature to 12 kHz at −150 °C and at −196 °C. Even at these low temperatures the line shape is a featureless single peak. This almost certainly rules out the possibility of H_3O^+ groups because these would give rise to a tripletlike line shape with a splitting of about 40 kHz.[58] However, it could still be possible that H_3O^+ groups do exist but randomly reorient at a rate faster than ~100 kHz, which would narrow the triplet to a single line. However, this is an unlikely possibility, because in other substances like H_3ONO_3 the H_3O^+ groups lose rapid rotational motion below −60 °C. The line width of our sample is constant between −150 and −196 °C, thus excluding the possibility of an onset of such motions at these temperatures. Therefore, we feel that the relatively small broadening of the resonance line at low temperatures negates the existence of H_3O^+ groups or any cluster of closely spaced protons, e.g., H_2O.

We can characterize much of the chemical environment of the hydrogens in $H_{0.3}Pt_3O_{3.25}Cl_{0.75}$ provided we know the magnitudes of the magnetic interactions that give rise to the observed line width of 8.4–12 kHz. The following possibilities have to be taken into account: (a) proton–proton homonuclear interactions, (b) heteronuclear interactions with ^{35}Cl and ^{37}Cl, (c) Knight shift, i.e., anisotropic interaction with conduction electrons, (d) anisotropic chemical shift, (e) interaction with paramagnetic centers, and (f) homogeneous broadening associated with molecular translation or motion. Several of these contributions have been evaluated in subsequent NMR experiments at room temperature. In a REV-8 experiment,[30] in which homonuclear interactions are decoupled, we obtained a spectrum corresponding to about 5 kHz. Thus, the contribution (a) from proton–proton dipolar broadening is of the order of 3 kHz. This agrees with a calculation of the second moment of the resonance line[59] in a model where 30% of the centers of the cubic sites in the bccub lattice of Pt_3O_4 are occupied, with $d = 5.76$ Å. The calculated second moment is 1.6 kHz^2, which for a Gaussian line shape corresponds to a line width of 3.0 kHz.

All static interactions (a–e) are suppressed in a multiple-pulse relaxation measurement.[31] The relaxation time measured under such conditions was $T_{1xz} = 40$ ms, corresponding to a negligibly small line width (f) of $1/\pi T_{1xz} = 8$ Hz. The paramagnetic susceptibility was determined by NMR to be 3.9×10^{-7} emu/g, which is too small to account for appreciable broadening due to paramagnetic centers (e).

Anisotropic Knight shifts and chemical shifts are indistinguishable. Similar proton NMR work[60] in $H_{1.7}MoO_3$ has shown that their combined effect in that system is a broadening of about 30 ppm or 2.7 kHz. However, these interactions do not dominate the line shapes in $H_xPt_3O_4$ because we do not observe the typical singularities of chemical shift tensor patterns.[29,60]

Heteronuclear broadening due to close proximity of ^{35}Cl and ^{37}Cl remains as the most likely candidate for the source of the residual broadening. For an H–Cl distance of 1.8 Å we predict[59] a dipolar interaction of the order of 5 kHz. This, combined with a chemical shift broadening of a few kHz and the 3.0-kHz homonuclear broadening, can explain the observed 12 kHz wide line at −150 °C.

The chemical model emerging from these observations consists of the $M_xPt_3O_4$ structure with 30% of the M sites occupied by H ions which are probably associated with Cl on O sites. The narrowing to 8.4 kHz at room temperature is evidence of the onset of rapid restricted motions of the hydrogen atoms.

Electrochemical Properties. Our investigation of platinum bronze electrodes has emphasized their interaction with O_2 because of its importance in fuel cells. If the rate of O_2 reduction to H_2O on Pt fuel-cell cathodes or on a Pt-substitute cathode could be improved, the economics of fuel-cell electric generators would become highly favorable.

In 0.1 N H_2SO_4 saturated with O_2 at 25 °C, the open-cell (rest) potentials for $Li_xPt_3O_4$, $Ni_xPt_3O_4$, and $Co_xPt_3O_4$ electrodes lie between 0.85 and 0.95 V vs. DHE. The potential is 100 mV lower for all electrodes in the same electrolyte saturated with N_2, which suggests that they are O_2 active. The N_2 values agree closely with the 0.75–0.8 V measured for Pt_3O_4 electrodes in 1 N H_2SO_4 by Sukhotin et al.[61] but are

(58) Andrew, E. R.; Behrson, R. *J. Chem. Phys.* **1950**, *18*, 159.

(59) Abragam, A. "Principles of Nuclear Magnetism"; Oxford University Press: London, 1961; Chapter IV.

(60) Taylor, R. D.; Ryan, L. M.; Tindall, P.; Gerstein, B. C. *J. Chem. Phys.* **1980**, *73*, 5500.

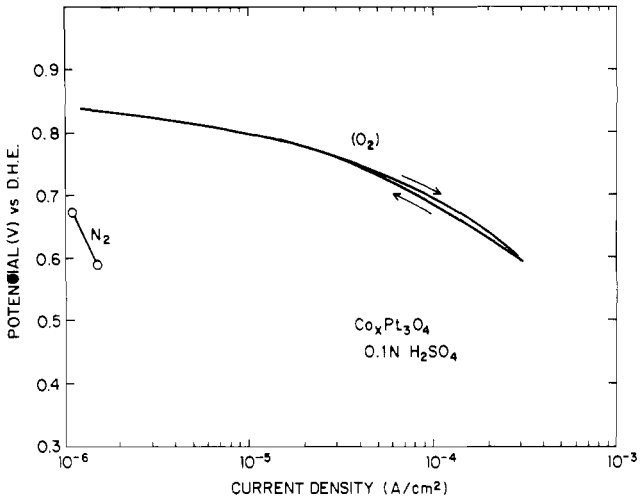

Figure 6. Oxygen reduction current vs. potential for a $Co_xPt_3O_4$ electrode in 0.1 N H_2SO_4 at 23 °C taken at a sweep rate of 0.1 mV/s.

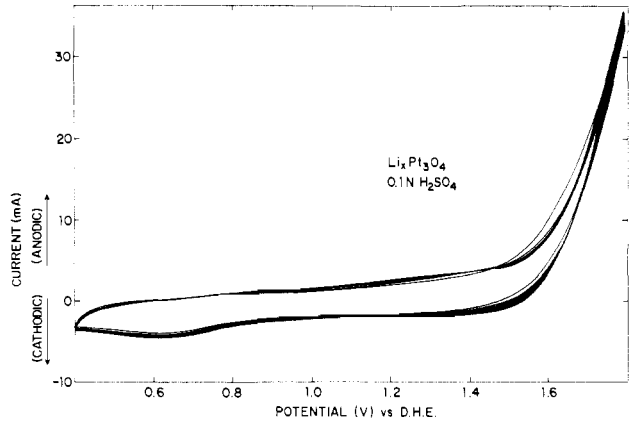

Figure 7. Voltammogram of a $Li_xPt_3O_4$ electrode measured at 20 mV/s sweep rate in 0.1 N H_2SO_4 saturated with N_2 at 23 °C.

below the standard potential of 1.11 V vs. NHE calculated by Nagel and Dietz[62] for a Pt-Pt_3O_4 couple. The measured potentials are substantially below the reversible O_2 potential of 1.23 V vs. NHE, corresponding to the O_2-H_2O reaction

$$O_2 + 4H^+ + 4e^- \rightleftarrows 2H_2O \text{ (1.23 V vs. NHE)}$$

They are also well below the 1.06 V vs. NHE mixed potential for Pt[63] and the 1.1 V vs. NHE measured for a Pt-O alloy electrode[64] and suggest that the platinum bronzes may have lower O_2 activity.

The electrocatalytic activity of the platinum bronzes for O_2 reduction has not previously been reported. We have measured high activity for $Li_xPt_3O_4$, $Ni_xPt_3O_4$, and $Co_xPt_3O_4$ electrodes. Figure 6 gives the current-voltage curve in O_2 and N_2 for a $Co_xPt_3O_4$ electrode swept between ~0.85 and 0.65 V vs. DHE at 0.1 mV/s. Similar results were obtained for $Li_xPt_3O_4$ and $Ni_xPt_3O_4$ electrodes. A general characteristic for the platinum bronze electrodes at high potential appears to be a small Tafel slope ($\sim dV/d \log i$) which increases at lower potentials. For the $Co_xPt_3O_4$ electrode the Tafel slope at high potential is ~50 mV/decade and increases rapidly below ~0.8 V to >150 mV/decade. These features are qualitatively similar to those for O_2 reduction on HNO_3-passivated Pt (Pt-O alloy) electrodes.[64] From capacitance estimates of electrode surface area, the O_2 reduction current density of platinum bronze electrodes is less than for bright Pt.

Figure 7 shows a voltammogram for $Li_xPt_3O_4$ obtained by sweeping the potential at 20 mV/s from 0.4 to 1.8 V vs. DHE. O_2 evolution commences at ~1.4 V, an anodic shoulder occurs at ~0.8 V, and a cathodic peak occurs in the vicinity of 0.65 V in the reverse sweep direction. The voltammogram is qualitatively similar to that measured for Pt_3O_4 by Sukhotin et al.[61] They attributed the cathodic peak to reduction of a surface-oxidized layer. When the $Li_xPt_3O_4$ electrode is swept to a less anodic potential of 1.0 V, no corresponding cathodic peak is detectable in the reverse sweep down to 0.4 V. It is thus likely that the cathodic peak for $Li_xPt_3O_4$ also corresponds to reduction of an oxidized surface layer.

Acknowledgment. We wish to thank C. M. Foris and G. A. Jones for assistance in obtaining the X-ray data, B. F. Burgess and C. R. Perrotto for atomic absorption analysis, J. L. Gillson for resistivity measurements, and A. Ferretti for preparation of some of the $Li_xPt_3O_4$ samples. We are especially grateful to I. McKinnon and C. E. Lyman for the SEM photographs and STEM analyses of $Ni_{0.46}Na_{0.21}Pt_3O_4$ and K. B. Schwartz for assistance in preparation of some of the samples of $Ni_xNa_yPt_3O_4$.

(61) Sukhotin, A. M.; Gankin, E. A.; Shalman, B. Y. *Zh. Prikl. Khim. (Leningrad)* **1972**, *45*, 1484.
(62) Nagel, K.; Dietz, H. *Electrochim. Acta* **1961**, *4*, 141.
(63) Hoare, J. D. *J. Electrochem. Soc.* **1979**, *126*, 1502.
(64) Hoare, J. P. *J. Electrochem. Soc.* **1965**, *112*, 849.

Contribution from the Chemistry Division, Argonne National Laboratory, Argonne, Illinois 60439

Synthesis and Characterization of Bis(μ-hydroxo)tetraaquadiplutonium(IV) Sulfate, $Pu_2(OH)_2(SO_4)_3 \cdot 4H_2O$, a Novel Compound Containing Hydrolyzed Plutonium(IV)[1]

DENNIS W. WESTER

Received January 20, 1982

$Pu_2(OH)_2(SO_4)_3 \cdot 4H_2O$ (I) has been synthesized by hydrothermal hydrolysis of plutonium(IV) sulfate solution. I forms as reddish orange crystals at 140 ± 5 °C. Analytical data for Pu (coulometric), SO_4^{2-} (gravimetric), and H_2O (thermogravimetric) are in agreement with theoretical values. X-ray powder diffraction data establish the isomorphicity of I with the Zr, Hf, and Ce analogues. Infrared spectra of I contain the peaks expected for hydroxo, aquo, and sulfato groups. Visible spectra of I are comparable to those for hydrated plutonium(IV) sulfate. Near-infrared spectra of I are reported. Comparisons between tetravalent hydroxysulfate compounds are made.

Hydrothermal hydrolysis of aqueous metal ions frequently leads to compounds with catenated or oligomeric species formed through hydroxo bridges. Among the more common examples are the polymeric hydroxysulfates $M(OH)_2SO_4 \cdot$

0020-1669/82/1321-3382$01.25/0